

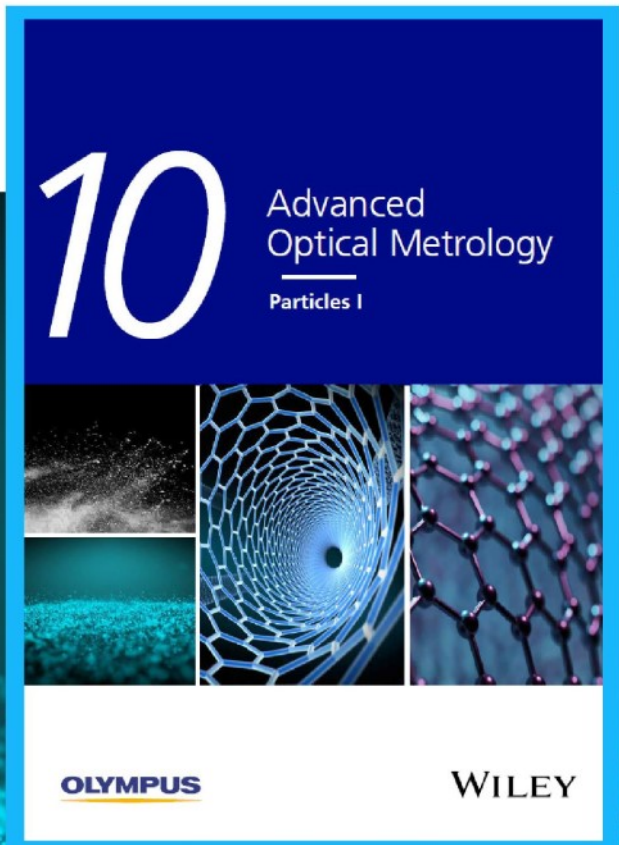


# Particles I

Access the latest eBook →

Particles: Unique Properties,  
Uncountable Applications

**Read the latest eBook and  
better your knowledge with  
highlights from the recent  
studies on the design and  
characterization of micro-  
and nanoparticles for  
different application areas.**



**Access Now**

This eBook is sponsored by

**OLYMPUS**

**WILEY**

# Mulberry-Leaves-Derived Red-Emissive Carbon Dots for Feeding Silkworms to Produce Brightly Fluorescent Silk

Jun Liu, Taoyi Kong, and Huan-Ming Xiong\*

Fluorescent silk has promising applications in dazzling textiles, biological engineering, and medical products, but the natural *Bombyx mori* silk has almost no fluorescence. Here carbon dots (CDs) made from mulberry leaves are reported, which have a strong near-infrared fluorescence with absolute quantum yield of 73% and a full width at half maximum of 20 nm. After feeding with such CDs, silkworms exhibit bright red fluorescence, grow healthily, cocoon normally, and turn to moths finally. The cocoons are pink in daylight and show bright red fluorescence under ultraviolet light. After breaking out of such cocoons, the red-emissive moths can mate and lay fluorescent eggs which would hatch normally. The growth cycle of the second generation of the test silkworm is the same as that of the control group, which means such CDs have excellent biocompatibility. Dissection and analyses on both the test silkworms and cocoons disclose the metabolic route of the CDs, that is, the fluorescent CDs are absorbed by silkworms from alimentary canals, then transferred to silk glands, and finally to cocoons, while those unabsorbed CDs are excreted with the feces. All experimental results confirm the excellent biocompatibility and fluorescence stability of such CDs.

## 1. Introduction

Fluorescent silk is a target of advanced material research for its promising applications in dazzling textiles, biological engineering, and medical products. Natural *Bombyx mori* silk has extraordinary biocompatibility and mechanical properties, but shows faint blue, pale yellow, or no fluorescence under ultraviolet (UV) light.<sup>[1–3]</sup> To obtain fluorescent *Bombyx mori* silk, genetic modification and dyeing with organic dyes have been developed in the past decade.<sup>[4,5]</sup> In general, genetic modification is an expensive and time-consuming work that may produce unexpected trouble to silkworm species, while production and use of organic dyes are always harmful to health and environment. Previous research has shown that feeding nanoparticles to small species can significantly change the properties of their bodies<sup>[6]</sup> or products.<sup>[7,8]</sup> Therefore, feeding silkworms with nontoxic, biocompatible, environmental benign, highly

luminescent, and low-cost substances seems to be the optimal strategy to produce fluorescent silk.<sup>[9–11]</sup>

Carbon dots (CDs) are the most competitive candidates for the above target, because they have shown outstanding biocompatibility and superior fluorescence in previous research such as bioimaging,<sup>[12,13]</sup> drug delivery,<sup>[14,15]</sup> and photothermal therapy.<sup>[16,17]</sup> In fact, many CDs are made from biomass, which guarantees the biosafety, low price, and green chemistry in CDs production.<sup>[18]</sup> In comparison with fluorescent organic dyes, rare earth nanoparticles, and semiconductor quantum dots, CDs would be the optimal choice for feeding silkworms. In 2019, blue-emissive CDs were first employed to feed silkworms, which produced blue-emissive silk with enhanced mechanical properties.<sup>[19]</sup> In the same year, blue-emissive CDs, CdSe/ZnS quantum dots, and rhodamine were fed to silkworms which produced

the corresponding blue, green and red fluorescent silk, respectively.<sup>[20]</sup> By far, CDs-derived fluorescent silk with longer emission wavelengths has not been reported yet. The reasons lie in the state of the art for CDs. On one hand, there are only a few reports about red-emissive CDs with both high quantum yield (QY) and narrow emission peaks, and even fewer red-emissive CDs that could be made in a large scale at low cost.<sup>[21–35]</sup> On the other, hydrophilic CDs are quickly discharged from the silkworm body and are not suitable for dyeing silkworms, while hydrophobic CDs are apt to accumulate excessively in the body and cause serious harm to silkworms,<sup>[10]</sup> because most of the hydrophobic CDs are made from aromatic compounds at present.<sup>[31,36]</sup> Therefore, it is really a challenge to synthesize hydrophobic red-emissive CDs from cheap biomass, which must adhere to the body and the silk of silkworms safely for a long time.

After screening many routes and carbon sources, we find a green and sustainable approach to prepare deep-red-emissive CDs (R-CDs) from mulberry leaves. The as-prepared CDs have a main emission peak at 676 nm with a shoulder at 725 nm, possessing an full width at half maximum (FWHM) of 20 nm and QY of 73%. They are the brightest deep-red-emissive CDs so far to our knowledge. Since their strong red fluorescence can be observed by naked eyes under a wide range of excitation wavelengths from UV to red, even in the sunlight, the R-CDs-fed silkworms can be monitored under the visible light irradiation safely. During several months' observation, these R-CDs-fed

J. Liu, T. Kong, H.-M. Xiong  
Department of Chemistry and Shanghai Key Laboratory of Molecular Catalysis and Innovative Materials  
Fudan University  
Shanghai 200438, P. R. China  
E-mail: hmxiong@fudan.edu.cn

 The ORCID identification number(s) for the author(s) of this article can be found under <https://doi.org/10.1002/adma.202200152>.

DOI: 10.1002/adma.202200152

silkworms grew healthily, wove cocoons, became moths, mated, and laid eggs. It is amazing that all these species, silkworms, cocoons, moths, and eggs are brightly luminescent! Such fluorescent eggs can be hatched for the next cycle of growth just like those in the control group, which strongly confirms the biocompatibility of R-CDs. In order to explore the distribution and metabolism of R-CDs in silkworms, the organs of silkworms were dissected and analyzed. The results showed that R-CDs could be partially metabolized through the silkworm excrement and partially transferred into silk glands and body walls through the alimentary canals. Finally, these absorbed R-CDs would enter into silk and form red-emissive shells of the cocoons.

## 2. Result and Discussion

Experimentally, fresh mulberry leaves were mashed and extracted with ethanol at first, and then the ethanol solution was heated in autoclaves at 150 °C for 4 h. After cooling down to room temperature, the solution was filtered and then dried by rotary evaporation, followed by extraction using a mixture of

dichloromethane and water with a volume ratio of 1:1. As shown in Figure 1a, the dried sample was separated into two parts: green-emissive CDs (G-CDs) in water and red-emissive CDs in dichloromethane. The aqueous solution of G-CDs is brown in the room light, only emitting green fluorescence under UV light (Figure 1b). In contrast, the R-CDs solution is dark green in the room light, which emits bright red fluorescence under UV, green and red light, respectively (Figure 1c). The absorption spectra in Figure 1d discloses the reason: G-CDs have only one absorption band at about 350 nm while R-CDs have a broad absorption band covering UV and visible regions. The photoluminescent (PL) emission spectra in Figure 1e shows that G-CDs have a broad emission band at about 500 nm, while R-CDs have a sharp emission peak at 676 nm with a shoulder at 725 nm. Such a sharp near-infrared emission is similar to that of R-CPDs made from taxus by Yang and co-workers,<sup>[37]</sup> but our preparation process needs neither dialysis nor silica column chromatography and thus has a high yield.<sup>[38]</sup> The FTIR spectra interpret the solubility difference between G-CDs and R-CDs (Figure 1f). Although two samples have similar vibrations of O–H/N–H ( $\approx 3700\text{--}3000\text{ cm}^{-1}$ ), C=O ( $\approx 1734\text{--}1653\text{ cm}^{-1}$ ), and C–N ( $\approx 1400\text{--}1330\text{ cm}^{-1}$ ) bonds, G-CDs show much stronger

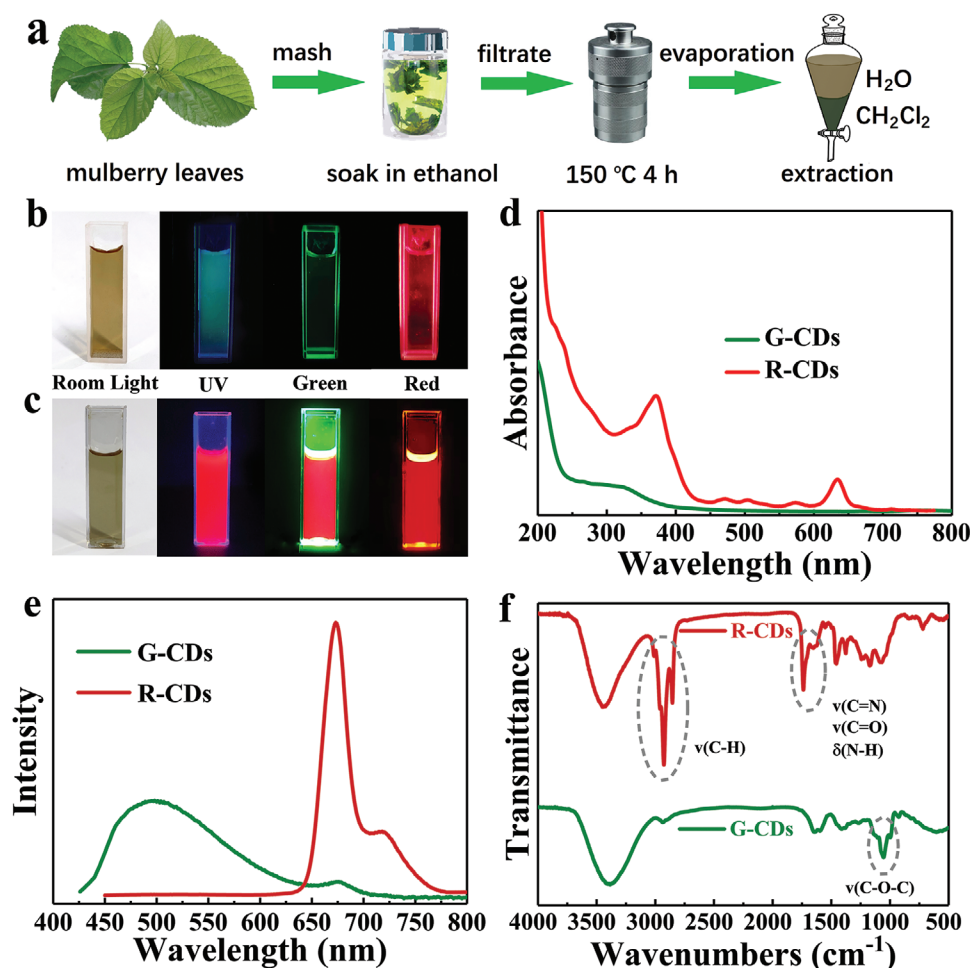


**Figure 1.** a) Synthesis and separation of CDs. b,c) Photos of CDs solutions under different irradiation light: b) G-CDs obtained from the above aqueous solution, and c) R-CDs obtained from the above  $\text{CH}_2\text{Cl}_2$  solution. d) Absorption spectra of G-CDs and R-CDs, respectively. e) PL emission spectra of G-CDs and R-CDs, respectively. f) FTIR spectra of G-CDs and R-CDs, respectively.

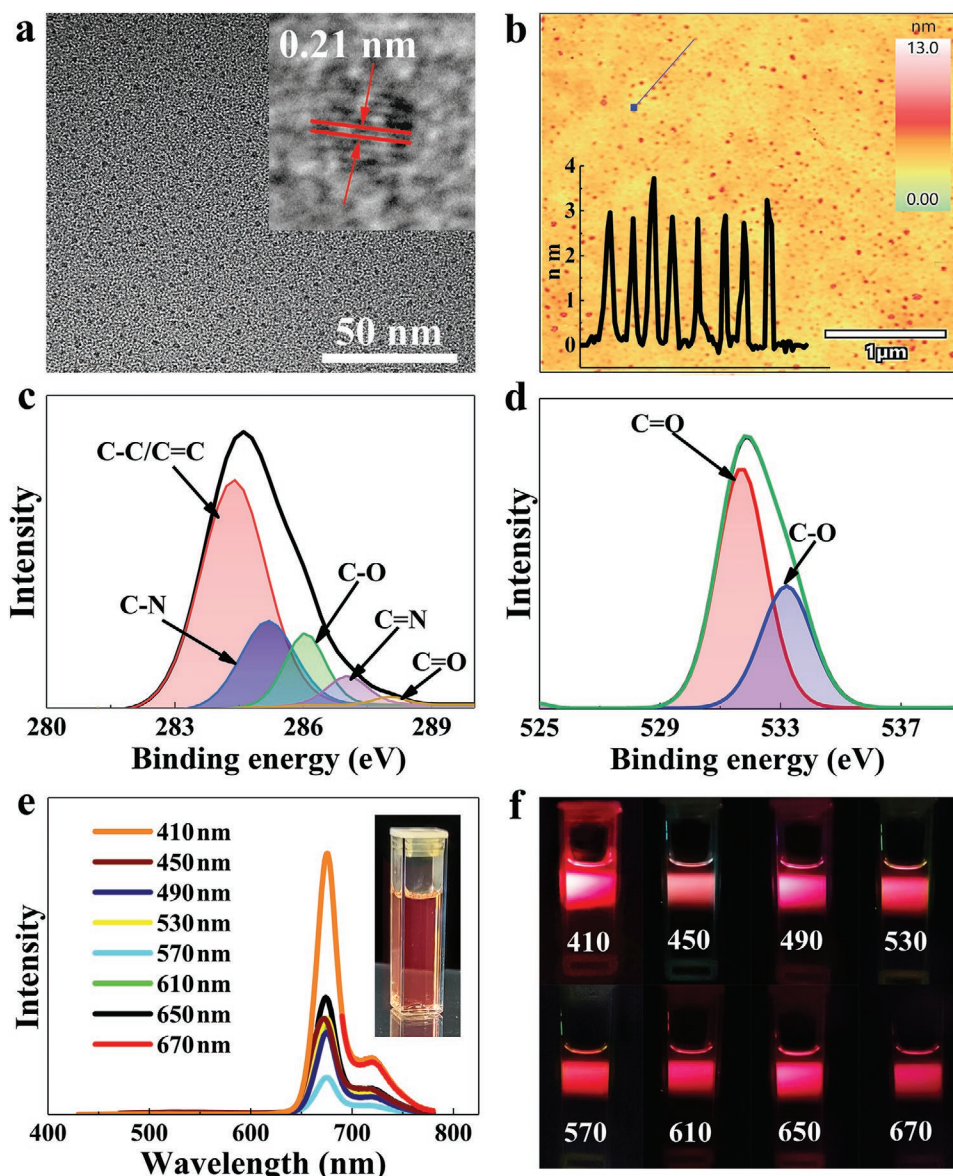


**Figure 2.** a) TEM and the inset HRTEM images of R-CDs. b) AFM image of R-CDs, and the inset histogram of height distribution of particles locating at the blue line. c) C1s XPS involving different carbon species and d) O1s XPS involving different oxygen species of R-CDs, respectively. e) PL emission spectra of R-CDs excited by different wavelengths of light, and the inset photo of an R-CDs solution in the sunlight. f) The R-CDs solution photos under different wavelengths of irradiation light, respectively.

IR bands of C–O–C at around  $1100\text{ cm}^{-1}$  which indicates their good solubility in water. In contrast, R-CDs exhibit a very strong IR band at  $\approx 3100\text{--}2800\text{ cm}^{-1}$ , representing the hydrophobic long alkyl chains and aromatic rings. In addition, R-CDs show significant C=C bonds in the aromatic ring skeleton at  $1610\text{ cm}^{-1}$ , stretching vibration of C=C bond at  $1460\text{ cm}^{-1}$  and the four consecutive  $\text{-CH}_2$  rocking vibrations at  $720\text{ cm}^{-1}$ . All these distinguished signals confirm the hydrophobicity of R-CDs. Moreover, the aromatic rings and large conjugated systems in R-CDs are the proofs for their significant absorption of visible light and their PL emission in near-infrared region.

Both the hydrophobicity and the near-infrared fluorescence of R-CDs are beneficial for feeding silkworms, and thus R-CDs are characterized in detail while the corresponding measure-

ments on G-CDs are deposited in the supporting information. The transmission electron microscopy (TEM) image of R-CDs in **Figure 2a** shows the monodispersed sample has a uniform size of about 3 nm, with the inset high-resolution TEM (HRTEM) image revealing a graphite lattice (100) distance of 0.21 nm. This result is identical with the histogram of R-CDs height distribution measured by the atomic force microscope (AFM) in **Figure 2b**. By fast Fourier transform (FFT) calculation, R-CDs have three lattice distances of 0.21, 0.24, and 0.34 nm, which correspond to the (100), (1120), and (002) planes of graphite, respectively (**Figure S1**, Supporting Information).<sup>[21,31,39–41]</sup> In contrast, the average particle size of G-CDs is slightly smaller than that of R-CDs, and no crystal lattices are found for G-CDs under HRTEM (**Figure S2**,

Supporting Information), which verifies again that R-CDs have a much higher graphitization degree than G-CDs, just like the above FTIR analyses. It is well known that the nanoparticle sizes measured by dynamic light scattering (DLS) are generally larger than those observed by TEM and AFM. Interestingly, the DLS results show that the evaluated size of R-CDs in ethanol solution is  $38 \pm 20$  nm, while that of G-CDs in aqueous solution is  $296 \pm 100$  nm (Figure S3, Supporting Information). This phenomenon can be ascribed to the organic chains on the CDs surfaces. G-CDs have a lower degree of carbonization, that is, there are more hydrophilic polymer chains on the surfaces, hence G-CDs adsorb plenty of water molecules to form larger hydration diameters than R-CDs.

The elemental composition and the chemical bond configurations of R-CDs and G-CDs are compared by X-ray photoelectron spectroscopy (XPS) measurements (Figure S4, Supporting Information, Figure 2c,d). According to the XPS survey data (Table S1, Supporting Information), the element composition of R-CDs is C (78.89%), N (0.27%), and O (20.84%), while that of G-CDs is C (67.92%), N (1.2%), and O (30.88%). On one hand, the carbon content in R-CDs is larger significantly, indicating that R-CDs have a higher carbonization degree. On the other, both nitrogen and oxygen contents in G-CDs are higher, suggesting their good hydrophilicity. The high-resolution XPS curves of C1s and O1s are deconvoluted for further analyses. For both R-CDs and G-CDs, the C1s spectra contain C–C/C=C (284.4 eV), C–N (285.2 eV), C–O (286 eV), C=N (287 eV), and C=O (288.2 eV), respectively, while the O1s spectra contain C=O (531.7 eV) and C–O (533.2 eV), respectively.<sup>[42,43]</sup> These results are in accordance with the above FTIR data. On the basis of TEM, FTIR, and XPS results, the red emission of R-CDs can be ascribed to their larger conjugated system and higher graphitization degree in comparison with G-CDs.

In the PL emission spectra of R-CDs, the sample exhibit a sharp peak at 676 nm with a shoulder at 725 nm (Figure 2e). The emission wavelength does not change when the excitation wavelength increases from 410 to 670 nm, which means the sample is not a mixture of different fluorescent matters. Such a strong deep-red emission can be clearly seen under different wavelengths of light (Figure 2f), even in the sunlight by naked eyes (inset of Figure 2e), indicating the high luminescent efficiency of R-CDs. The absolute QY of R-CDs were measured by an integrating sphere carefully (Figure S5, Supporting Information), for which R-CDs were dissolved in ethanol with an absorbance value below 0.1 at the optimal excitation wavelength of 406 nm. Under this condition, the PLQY was measured to be 72.6%. When the excitation wavelength was changed to be 510 nm, the QY was measured to be 41.4%, indicating the silkworms fed with R-CDs could show considerable fluorescence under green light. In comparison with those extensively cited literatures, both the QY and the FWHM of our R-CDs are outstanding among the reported red-emissive CDs (Table S2, Supporting Information). Furthermore, among those highly red-emissive CDs, only a few samples were made from biomass which could guarantee eco-safety.<sup>[37]</sup> In brief, all the merits including near-infrared emission, high QY, narrow FWHM, good hydrophobicity, and biosafety, endow the mission of feeding silkworms to our R-CDs.

Hundreds of silkworms were fed with ordinary fresh mulberry leaves until the second day of the fifth instar, among which 120 silkworms with similar body weight were picked out for the following experiments. 20 silkworms were set as control and fed as before, while the others were fed with mulberry leaves sprayed with R-CDs solutions of different concentrations, respectively. All of the silkworms grew healthily under very careful treatment till cocooning (Figure S7, Supporting Information), with a maintained humidity of 60% at 25 °C. After a 24 h fast, the silkworms in the test group were studied under green light irradiation. In Figure 3a-i, bright red fluorescence can be seen from the whole body of the silkworm by naked eyes. Through the filter of an automatic stereo fluorescence microscope, the images of the abdomen (Figure 3a-ii), the head and the thorax (Figure 3a-iii) show the red fluorescence mainly located at the dorsal blood vessels and both sides of the thorax of the silkworm. In the fluorescence video (supporting information), the silkworm is moving freely and emitting brightly red fluorescence in its whole body, which was recorded by a camera through a filter under green light irradiation. This phenomenon can be seen in Figure S8, Supporting Information, even when the silkworms are cocooning. In contrast, the silkworms in the control group exhibits no obvious fluorescence under the green light irradiation (Figure S8d, Supporting Information). Only under the UV light irradiation, faint yellowish fluorescence can be seen at their four pairs of abdominal legs and the junction of the abdominal segment after the fifth abdominal segment (Figure 3b).

Although these silkworms were divided into 6 groups and fed with different amounts of R-CDs respectively, all silkworms grew steadily in the fifth instar and their weights are close to each other (Figure 3c). No silkworms died during this period, and all of them could cocoon normally after the fifth instar, which verifies the biosafety of our R-CDs. The UV-vis absorption spectra and PL spectra of different silkworm body walls are compared in Figure 3d,e. The absorption curve of the silkworm body wall in the test group has two peaks at 406 and 660 nm respectively, while that of the control group shows no significant peaks. In the PL spectra, the test group exhibits the same R-CDs emission features, while the control group shows very weak yellow-green emission. These results confirm that R-CDs did not change after intake on one hand, and on the other, the silkworms in the fifth instar have almost no background fluorescence under green light irradiation, which is beneficial for further bioimaging research.

The cocoons of all test groups are pink in the daylight and emit red fluorescence under UV light (Figure 3f). After creeping out of the cocoons, the silkworm moths also exhibit weak red fluorescence under UV light (Figure 3g). These results suggest that the R-CDs fed to silkworms have been successfully ingested and expressed in cocoons and even in moths. More importantly, the cocoon-breaking moths in the test groups could mate and reproduce normally. Their eggs could hatch out normally, and the newborn healthy silkworms could grow and reproduce like their ancestors (Figure 3h,i). These results confirm the excellent biocompatibility of our R-CDs undoubtedly (Figure S9, Supporting Information). It should be mentioned that the cocoons in the control group appear light pink in daylight, and have almost no fluorescence under the UV lamp (Figure S10, Supporting Information).

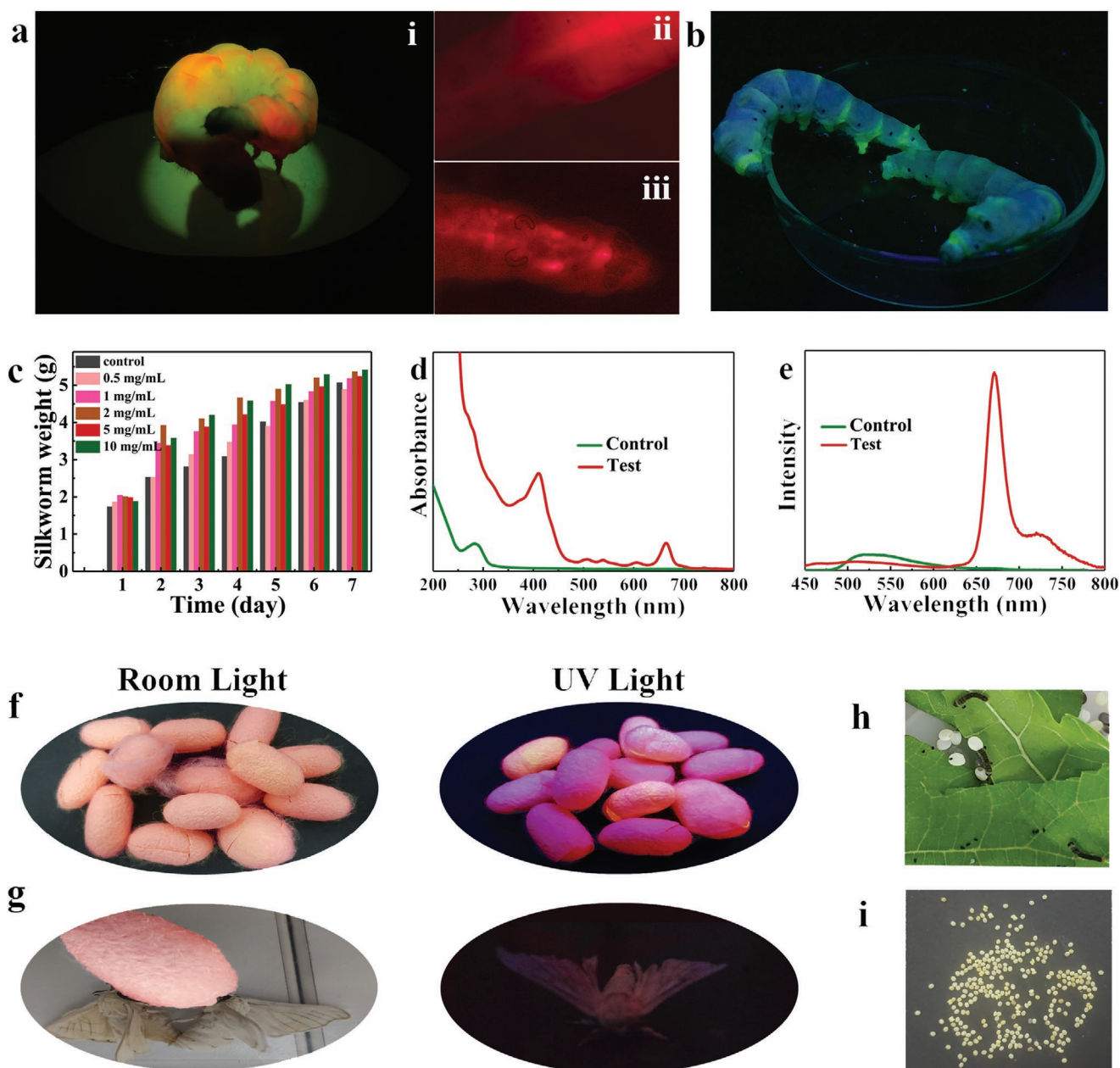


**Figure 3.** a) Photographs of a silkworm in the test group: i) the whole body under green light, ii) the head, and iii) the chest under an automatic stereo fluorescence microscope (filtering out the green excitation light). b) The silkworms in the control group under UV light. c) Weight changes of silkworms fed with different concentrations of R-CDs, from the second day of the 5th instar to cocooning (normalized to weight,  $n = 20$ ). Data are expressed as means  $\pm$  SD. Differences were assessed by one-way analysis of variance (ANOVA) followed by Tukey's multiple comparison test.  $***P < 0.001$ ,  $**P < 0.01$ ,  $*P < 0.05$ . d) UV-vis absorption curves and e) PL emission spectra of the silkworm body wall in the control and the test group, respectively. f) Cocoons of and g) silkworm moths of the test group in daylight and UV light, respectively. h) The second-generation silkworms hatched out from the eggs. i) Eggs photo under room light, which are laid by the silkworm moths of the second-generation.

To find the fluorescence origin, both the cocoons and the silkworm feces were extracted by ethanol and analyzed by the fluorescent techniques, respectively. After dissection, a silkworm cocoon has three parts: the coat, the shell, and the lining. Under the UV light, both the coat and the shell of the test group are red-emitting, while the lining is yellow emitting. On the contrary, all three parts of the control group show very weak yellowish fluorescence or no fluorescence (Figure S10,

Supporting Information). The ethanol solutions of the above parts have the same PL features as they are observed under UV light. Both the cocoon coats and the cocoon shells in the test group show the same PL spectra as that of R-CDs (Figure 4a). The TEM images of their ethanol solutions are also similar to those of R-CDs (Figure 4b). Obviously, the red fluorescence of these two parts originates from the ingested R-CDs. In contrast, the PL spectra of the control cocoons extraction are

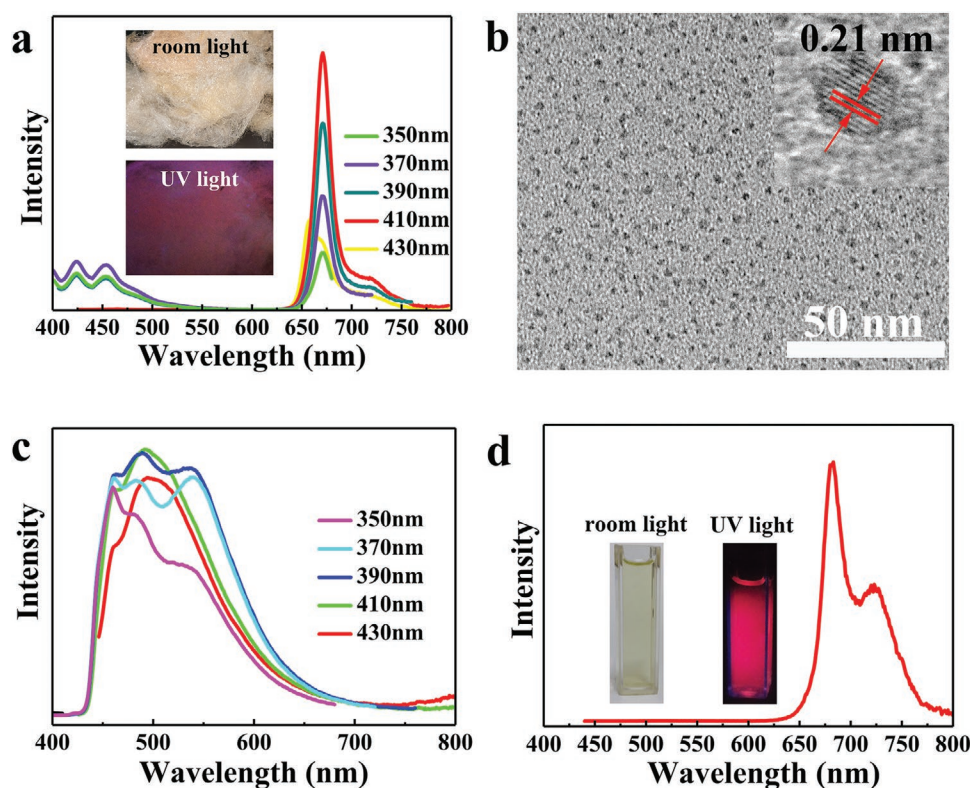


**Figure 4.** a) The PL emission spectra of the ethanol solution extracted from the cocoon coats and the cocoon shells in the test group, under different wavelengths of excitation light. Inset photos: the cocoon coats under the room light and in UV light. b) TEM and the inset HRTEM images of the ethanol extraction of cocoon coats. c) PL emission spectra of the ethanol solution extracted from the cocoon coats and the cocoon shells in the control group, under different wavelengths of excitation light. d) PL emission spectra of the ethanol solution extracted from the silkworm feces in the test group. Inset photos: the above ethanol solution under the room light (left) and the UV light (right).

complicated, exhibiting a very broad emission band with multi peaks (Figure 4c). And the PL emission bands vary constantly when the excitation wavelength changes. This phenomenon indicates that the natural cocoons have complex fluorescent components, but fortunately these components show very weak emissions that do not interfere with the strong emission of R-CDs. As for the feces of silkworms, the ethanol extraction of the test group is red-emitting under UV light and shows the R-CDs PL features (Figure 4d), which indicates R-CDs have passed through the whole alimentary canal but not been absorbed completely.

After feeding with R-CDs for 7 days and one day of fasting, a mature silkworm in the 5th instar was dissected under a UV light. As shown in Figure 5a and Figure S12, Supporting Information, the alimentary canal, the anterior and the middle silk glands emit bright red fluorescence, while both the rear silk gland and the urinary system emit bright yellow fluorescence. The alimentary canal of the control group (Figure 5b) looks green in daylight and shows weak yellow-green fluorescence under UV light. In contrast, the alimentary canal of the test group looks yellow in daylight, with some gray-green areas (Figure 5c). Under the UV lamp, the fluorescent color of this alimentary canal turns from red (top) to yellow (bottom). According to previous reports, the yellow fluorescence is owing to flavonoid glycosides in mulberry leaves.<sup>[44–51]</sup> Obviously, the red-fluorescence distribution indicates that R-CDs are probably

absorbed into the body through the second half of the alimentary canal (Figure 5d). To verify this hypothesis, the midgut of the test group was cleaned thoroughly and then broken by an ultrasonic cell disruption system. The sample was extracted with ethanol for TEM observation. In Figure 5e, both the TEM image and the inset HRTEM images confirm the existence of R-CDs in the midgut. Furthermore, both the UV-vis absorption (Figure 5f) and the PL emission (Figure 5g) spectra of the test group are similar to those of R-CDs, while the extraction of the control groups shows a rather weak absorption and yellow fluorescence.

In daylight and UV light, the silk glands of the silkworms in the test group look red and yellow in different areas respectively, while the silk glands of the silkworms in the control group are nearly transparent and colorless (Figure S13, Supporting Information). Since the anterior and middle silk glands emit red fluorescence in UV light, this part was broken in an ethanol solution of  $\text{CaCl}_2$ . The resulting solution was concentrated and dried by rotary evaporation, followed by extraction of petroleum ether, and finally dispersed in ethanol. Both TEM and HRTEM images in Figure 5h show that the as-obtained sample is similar to R-CDs and that extracted from the midgut. In addition, the UV-vis absorption (Figure 5i) and the PL emission (Figure 5j) spectra are also similar to those of R-CDs, respectively. Therefore, both TEM and PL analyses prove that one metabolic route of the R-CDs digested

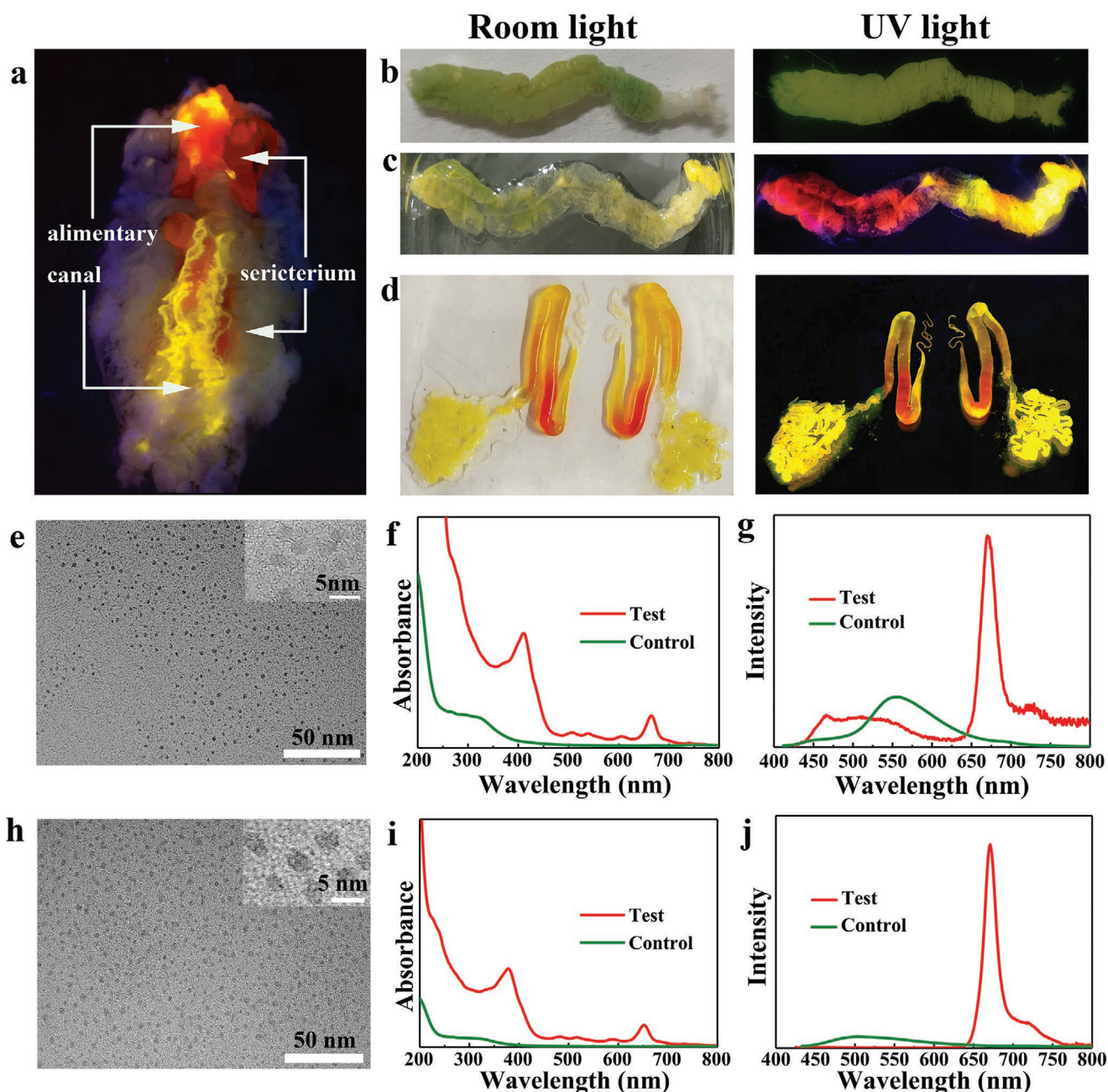


**Figure 5.** a) A full anatomical picture of a silkworm in the test group under UV light. b) The alimentary canal of the control group, c) the alimentary canal of the test group, and d) the silk glands of the test group were photographed in daylight (left) and UV light (right), respectively. e) TEM and the inset HRTEM images of the alimentary canal extract from the test group. f) The UV-vis absorption curves of the sample and the control. g) PL emission spectra of the sample and the control. h) TEM and the inset HRTEM images of the silk gland extract from the test group. i) The UV-vis absorption curves of the sample and the control. j) PL emission spectra of the sample and the control.

and absorbed by silkworms is from alimentary canals to silk glands, and finally to cocoons. It should be mentioned that the alimentary canals of both the test and the control groups show yellow fluorescence as reported before, but in the silk glands and the cocoon lining, only the test group have significant yellow fluorescence. This phenomenon might be ascribed to some stress reactions caused by the intake of R-CDs, which leak the yellow-emissive flavonoid glycosides from alimentary canals to silk glands.<sup>[52,53]</sup>

### 3. Conclusion

Near-infrared-emissive CDs were fed to silkworms safely to produce brightly luminescent natural silk. The silkworm bodies, alimentary canals, silk glands, feces, cocoons, and moths are red fluorescent with the spectral features of R-CDs, and R-CDs can be separated from the above tissues. Therefore, the physiological activities of the test silkworms can be monitored by fluorescence imaging, even be seen by naked eyes. The test group

grew healthily, developed normally, mated, and laid eggs that could hatch to produce the next generation. All these achievements are based on the merits of our R-CDs, including NIR emission above 700 nm, high QY of 73%, narrow FWHM of 20 nm, good hydrophobicity, and excellent biocompatibility. Since such R-CDs can be easily prepared from mulberry leaves on large scale and the fed silkworms have a survival rate of nearly 100%, the fluorescent *Bombyx mori* silk will have a mass production for practical applications in the future.

## Supporting Information

Supporting Information is available from the Wiley Online Library or from the author.

## Acknowledgements

This work was financially supported by the National Natural Science Foundation of China (21975048, 21771039), and the Shanghai Science and Technology Committee (19DZ2270100). All animal experiments were performed in accordance with the Guide for the Care and Use of Laboratory Animals and approved by the Department of Laboratory Animal Science at Fudan University (Shanghai, P. R. China) with the approval number 202201004Z.

## Conflict of Interest

The authors declare no conflict of interest.

## Data Availability Statement

The data that support the findings of this study are available from the corresponding author upon reasonable request.

## Keywords

biocompatibility, carbon dots, feeding silkworms, fluorescent silk, near infrared fluorescence

Received: January 7, 2022  
Revised: February 19, 2022  
Published online: March 15, 2022

- [1] F. G. Omenetto, D. L. Kaplan, *Science* **2010**, *329*, 528.
- [2] C. Patra, S. Talukdar, T. Novoyatleva, S. R. Velagala, C. Muehlfeld, B. Kundu, S. C. Kundu, F. B. Engel, *Biomaterials* **2012**, *33*, 2673.
- [3] B. Kundu, S. C. Kundu, *Biomaterials* **2012**, *33*, 7456.
- [4] T. Tamura, C. Thilbert, C. Royer, T. Kanda, E. Abraham, M. Kamba, N. Komoto, J. L. Thomas, B. Mauchamp, G. Chavancy, P. Shirk, M. Fraser, J. C. Prudhomme, P. Couble, *Nat. Biotechnol.* **2000**, *18*, 81.
- [5] C. R. Holkar, A. J. Jadhav, D. V. Pinjari, N. M. Mahamuni, A. B. Pandit, *J. Environ. Manage.* **2016**, *182*, 351.
- [6] A. Pluskota, E. Horzowski, O. Bossinger, A. von Mikecz, *PLoS One* **2009**, *4*, e6622.
- [7] E. Lepore, F. Bosia, F. Bonaccorso, M. Bruna, S. Taioli, G. Garberoglio, A. C. Ferrari, N. M. Pugno, *2D Mater.* **2017**, *4*, 031013.
- [8] Q. Wang, C. Wang, M. Zhang, M. Jian, Y. Zhang, *Nano Lett.* **2016**, *16*, 6695.
- [9] N. C. Tansil, Y. Li, C. P. Teng, S. Zhang, K. Y. Win, X. Chen, X. Y. Liu, M. Y. Han, *Adv. Mater.* **2011**, *23*, 1463.
- [10] N. C. Tansil, Y. Li, L. D. Koh, T. C. Peng, K. Y. Win, X. Y. Liu, M. Y. Han, *Biomaterials* **2011**, *32*, 9576.
- [11] X. Zheng, M. Zhao, H. Zhang, S. Fan, H. Sha, X. Hu, Y. Zhang, *ACS Biomater. Sci. Eng.* **2018**, *4*, 4021.
- [12] B. Wu, K. Li, F. Sun, J. Niu, R. Zhu, Y. Qian, S. Wang, *Adv. Healthcare Mater.* **2021**, *10*, 2100512.
- [13] D. Li, P. Jing, L. Sun, Y. An, X. Shan, X. Lu, D. Zhou, D. Han, D. Shen, Y. Zhai, S. Qu, R. Zboril, A. L. Rogach, *Adv. Mater.* **2018**, *30*, 1705913.
- [14] B. Geng, P. Li, F. Fang, W. Shi, J. Glowacki, D. Pan, L. Shen, *Carbon* **2021**, *184*, 375.
- [15] S. Li, W. Su, H. Wu, T. Yuan, C. Yuan, J. Liu, G. Deng, X. Gao, Z. Chen, Y. Bao, F. Yuan, S. Zhou, H. Tan, Y. Li, X. Li, L. Fan, J. Zhu, A. T. Chen, F. Liu, Y. Zhou, M. Li, X. Zhai, J. Zhou, *Nat. Biomed. Eng.* **2020**, *4*, 704.
- [16] X. Bao, Y. Yuan, J. Chen, B. Zhang, D. Li, D. Zhou, P. Jing, G. Xu, Y. Wang, K. Hala, D. Shen, C. Wu, L. Song, C. Liu, R. Zboril, S. Qu, *Light: Sci. Appl.* **2018**, *7*, 91.
- [17] Y. Li, G. Bai, S. Zeng, J. Hao, *ACS Appl. Mater. Interfaces* **2019**, *11*, 4737.
- [18] W. Meng, X. Bai, B. Wang, Z. Liu, S. Lu, B. Yang, *Energy Environ. Mater.* **2019**, *2*, 172.
- [19] S. Fan, X. Zheng, Q. Zhan, H. Zhang, H. Shao, J. Wang, C. Cao, M. Zhu, D. Wang, Y. Zhang, *Nano-Micro Lett.* **2019**, *11*, 75.
- [20] L. Cheng, H. Zhao, H. Huang, B. Li, R. K. Y. Li, X. Q. Feng, F. Dai, *J. Mater. Sci.* **2019**, *54*, 9945.
- [21] Y. Ru, L. Sui, H. Song, X. Liu, Z. Tang, S. Q. Zang, B. Yang, S. Lu, *Angew. Chem., Int. Ed.* **2021**, *60*, 14091.
- [22] X. Q. Niu, T. B. Song, H. M. Xiong, *Chin. Chem. Lett.* **2021**, *32*, 1953.
- [23] Q. Zhao, W. Song, B. Zhao, B. Yang, *Mater. Chem. Front.* **2020**, *4*, 472.
- [24] C. L. Shen, Q. Lou, J. H. Zang, K. K. Liu, S. N. Qu, L. Dong, C. X. Shan, *Adv. Sci.* **2020**, *7*, 1903525.
- [25] H. Ding, X. X. Zhou, J. S. Wei, X. B. Li, B. T. Qin, X. B. Chen, H. M. Xiong, *Carbon* **2020**, *167*, 322.
- [26] H. Ding, X. H. Li, X. B. Chen, J. S. Wei, X. B. Li, H. M. Xiong, *J. Appl. Phys.* **2020**, *127*, 231101.
- [27] B. Wang, Y. Yu, H. Zhang, Y. Xuan, G. Chen, W. Ma, J. Li, J. Yu, *Angew. Chem., Int. Ed.* **2019**, *58*, 18443.
- [28] B. Wang, J. Li, Z. Tang, B. Yang, S. Lu, *Sci. Bull.* **2019**, *64*, 1285.
- [29] X. Shi, H. Meng, Y. Sun, L. Qu, Y. Lin, Z. Li, D. Du, *Small* **2019**, *15*, 1901507.
- [30] F. Li, Y. Li, X. Yang, X. Han, Y. Jiao, T. Wei, D. Yang, H. Xu, G. Nie, *Angew. Chem., Int. Ed.* **2018**, *57*, 2377.
- [31] H. Ding, J. S. Wei, P. Zhang, Z. Y. Zhou, Q. Y. Gao, H. M. Xiong, *Small* **2018**, *14*, 1800612.
- [32] J. Shao, S. Zhu, H. Liu, Y. Song, S. Tao, B. Yang, *Adv. Sci.* **2017**, *4*, 1700395.
- [33] S. Lu, L. Sui, J. Liu, S. Zhu, A. Chen, M. Jin, B. Yang, *Adv. Mater.* **2017**, *29*, 1603443.
- [34] H. Ding, J. S. Wei, N. Zhong, Q. Y. Gao, H. M. Xiong, *Langmuir* **2017**, *33*, 12635.
- [35] H. Ding, S. B. Yu, J. S. Wei, H. M. Xiong, *ACS Nano* **2016**, *10*, 484.
- [36] F. Yuan, T. Yuan, L. Sui, Z. Wang, Z. Xi, Y. Li, X. Li, L. Fan, Z. a. Tan, A. Chen, M. Jin, S. Yang, *Nat. Commun.* **2018**, *9*, 2249.
- [37] J. Liu, Y. Geng, D. Li, H. Yao, Z. Huo, Y. Li, K. Zhang, S. Zhu, H. Wei, W. Xu, J. Jiang, B. Yang, *Adv. Mater.* **2020**, *32*, 1906641.
- [38] S. Ghosh, H. Ali, N. R. Jana, *ACS Sustainable Chem. Eng.* **2019**, *7*, 12629.
- [39] J. Peng, W. Gao, B. K. Gupta, Z. Liu, R. Romero-Aburto, L. Ge, L. Song, L. B. Alemany, X. Zhan, G. Gao, S. A. Vithayathil,

- B. A. Kaiparettu, A. A. Marti, T. Hayashi, J. J. Zhu, P. M. Ajayan, *Nano Lett.* **2012**, *12*, 844.
- [40] Y. Zhang, C. W. Foster, C. E. Banks, L. Shao, H. Hou, G. Zou, J. Chen, Z. Huang, X. Ji, *Adv. Mater.* **2016**, *28*, 9391.
- [41] Y. Li, Y. Zhao, H. Cheng, Y. Hu, G. Shi, L. Dai, L. Qu, *J. Am. Chem. Soc.* **2012**, *134*, 15.
- [42] Y. Dong, H. Pang, H. B. Yang, C. Guo, J. Shao, Y. Chi, C. M. Li, T. Yu, *Angew. Chem., Int. Ed.* **2013**, *52*, 7800.
- [43] J. Wang, F. Peng, Y. Lu, Y. Zhong, S. Wang, M. Xu, X. Ji, Y. Su, L. Liao, Y. He, *Adv. Opt. Mater.* **2015**, *3*, 103.
- [44] L. Hu, C. Wang, X. Guo, D. Chen, W. Zhou, X. Chen, Q. Zhang, *Front. Plant Sci.* **2021**, *12*, 684974.
- [45] M. S. Butt, A. Nazir, M. T. Sultan, K. Schroen, *Trends Food Sci. Technol.* **2008**, *19*, 505.
- [46] K. Doi, T. Kojima, M. Makino, Y. Kimura, Y. Fujimoto, *Chem. Pharm. Bull.* **2001**, *49*, 151.
- [47] Z. Jia, M. C. Tang, J. M. Wu, *Food Chem.* **1999**, *64*, 555.
- [48] Y. Zhang, X. Yu, W. Shen, Y. Ma, L. Zhou, N. Xu, S. Yi, *Sci. China: Life Sci.* **2010**, *53*, 1330.
- [49] D. Li, G. Chen, B. Ma, C. Zhong, N. He, *J. Agric. Food Chem.* **2020**, *68*, 1494.
- [50] W. T. Ju, O. C. Kwon, H. B. Kim, G. B. Sung, H. W. Kim, Y. S. Kim, *J. Food Sci. Technol.* **2018**, *55*, 1789.
- [51] X. Y. Chen, T. Zhang, X. Wang, M. T. Hamann, J. Kang, D. Q. Yu, R. Y. Chen, *Molecules* **2018**, *23*, 1018.
- [52] H. Y. Wang, S. F. Zhou, M. Zhang, H. D. Wang, Y. Q. Zhang, *J. Biomed. Mater. Res., Part A* **2022**, *110*, 827.
- [53] C. Offord, F. Vollrath, C. Holland, *J. Mater. Sci.* **2016**, *51*, 10863.